Temporal relaxation of excited-level populations of atoms and ions in a plasma: Validity range of the quasi-steady-state solution of coupled rate equations

Keiji Sawada and Takashi Fujimoto
Department of Engineering Science, Kyoto University, Kyoto 606-01, Japan
(Received 22 October 1993)

By solving the coupled rate equations for excited level populations for an abrupt change of plasma parameters, we have examined the transient characteristics of these populations which approach the steady-state values with time. For hydrogen atoms under the ionizing plasma condition the transient time of the levels lying lower than Griem's boundary, i.e., the level at which the radiative and collisional depopulation rates are equal, is determined by their natural lifetimes, and that of all the higher-lying levels is given by the relaxation time of the boundary level. Under the recombining plasma condition the transient time of the levels lying higher than the boundary is determined by their own relaxation times, and that of the lower-lying levels is given by that of the boundary level. Thus, the overall response of excited level populations is determined by the relaxation time of Griem's boundary level. The effective rates for ionization and recombination are also examined.

PACS number(s): 52.25.Jm, 32.70.−n, 34.10.+x, 52.70.−m

I. INTRODUCTION

Spectroscopy of radiation emitted from a plasma is a powerful technique for studying the nature of the plasma. Emission lines constitute the dominant part of the spectrum, and intensity of a line corresponds to the excited-level population of atoms or ions. The population distribution over their excited levels is determined by the collisional and radiative processes taking place in the plasma.

We take hydrogen atoms as an example in the following study. We assume that levels are distinguished by their principal quantum number p. The temporal development of population $n(p)$ is described by the rate equation,

$$dn(p)/dt=\sum_{q<p}C(q,p)n_e n(q)+\sum_{q>p}[F(q,p)n_e+A(q,p)]n(q)+[\alpha(p)n_e+\beta(p)]n_z n_e - \left[\left[\sum_{q<p}F(p,q)+\sum_{q>p}C(p,q)+S(p)\right]n_e+\sum_{q<p}A(p,q)\right]n(p) \quad (p=1,2,3,\ldots), \tag{1}$$

which is coupled with similar equations for other levels. Here $C(p,q)$ and $F(q,p)$ are the excitation rate coefficient by electron collisions from state p to q and its inverse deexcitation rate coefficient, respectively, $A(q,p)$ is the spontaneous transition probability from q to p, $S(p)$ and $\alpha(p)$ are the ionization rate coefficient and the three-body recombination rate coefficient, respectively, and $\beta(p)$ is the radiative recombination rate coefficient. We assume that the electron density n_e, ion density n_z, and the electron temperature T_e are given. Thus we have a set of coupled differential equations, and, in principle, we have to solve it under a given plasma condition. The quantity in the large square brackets in the second line of the right-hand side of Eq. (1), i.e., the total depopulation rate of level p, is the inverse *relaxation time*, $\tau(p)^{-1}$, of this level.

More than 30 years ago the collisional-radiative (CR) model, or more specifically, the method of the quasi-steady-state (QSS) solution, was proposed [1–3] for the set of rate equations (1). According to this method, Eq. (1) is set equal to zero for excited levels:

$$dn(p)/dt=0 \quad (p=2,3,4,\ldots), \tag{2}$$

resulting in a set of coupled linear equations for these levels. These equations are readily solved in the form

$$n(p)=R_0(p)n_z n_e+R_1(p)n(1)n_e \quad (p=2,3,4,\ldots), \tag{3}$$

where $R_0(p)$ and $R_1(p)$ are functions of n_e and T_e.

The rate equation, Eq. (1), for the ground state is rewritten in terms of $R_0(p)$ and $R_1(p)$ for $p\geq 2$, viz.,

$$dn(1)/dt=-S_{\mathrm{CR}}n(1)n_e+\alpha_{\mathrm{CR}}n_z n_e, \tag{4}$$

where S_{CR} and α_{CR} are the collisional-radiative ionization and recombination rate coefficients, respectively, and functions of n_e and T_e.

The QSS has been extensively used in interpreting the observed spectral line intensities from various plasmas. QSS proved useful also in understanding the general

characteristics of the population kinetics of excited levels [4–8].

Reference [1] gives the validity conditions of the QSS approximation, viz.,

$$n(p) \ll n_e \quad \text{and} \quad n(p) \ll n(1) \quad (p=2,3,4,\dots) . \tag{5}$$

The authors say "In such plasma a quasiequilibrium number density of excited system is established almost instantaneously without the number densities of free electrons and bare nuclei being appreciably altered." They continue "An instructive complementary description of the situation is that the relaxation times for the excited levels are very much shorter than the relaxation time for the ground levels or for the free electrons." In addition to Eq. (5), they require that "the life of an electron in any level of importance exceeds the time the electron takes to describe its orbit."

With regard to the validity of QSS, Limbaugh and Mason took helium and examined the validity by calculating the temporal development of the excited-level populations [9]. However, the helium system has metastable levels, which have exceptionally long relaxation times and their plasma conditions were rather limited. Thus their result turns out not to be useful to predict the validity of QSS in more general situations.

Recently, plasmas under rapidly changing conditions have become realized, in which the approximation of QSS may be violated or the transient characteristics of the populations, before they reach the QSS values, are essential. Examples are the neutral beam particles injected into a plasma, which experience a rapid change in plasma conditions, and rapidly cooled laser produced plasmas. For the latter plasmas, several theoretical studies are reported, in which the rate equations are numerically solved and the population inversion density and the laser gain are presented for the purpose of examining performance of the short wavelength lasers on hydrogenlike ions [10–17]. However, little attention has been paid to the transient characteristics of the populations.

In view of the above situations it appears desirable to examine systematically the transient characteristics of the excited-level populations before they reach the QSS values, and on the basis of these characteristics, to present the validity criterion for the QSS approximation.

II. TRANSIENT POPULATIONS AND TRANSIENT TIME OF EXCITED LEVELS

The right-hand side of Eqs. (3) contains, as parameters, $n(1)$ and n_z as well as n_e and T_e. The approximation, Eq. (2), corresponds to the assumption that the population densities of excited levels adjust themselves instantaneously to the changing $n(1)$, n_z, n_e, and T_e. However, each of the excited levels should have a finite response time to these parameters. In the following, in order to see the response of the excited-level populations, we solve the set of Eq. (1) under typical conditions without the QSS assumption.

The atomic data used are given in Refs. [18,19]. We solve the populations for $2 \le p \le 35$. The populations for $36 \le p \le 76$ are given appropriate values on the basis of reasonable approximations depending on the particular situations. The limit $p=76$ corresponds to the last bound level under our condition of $n_e = 10^{12}$ cm^{-3}; this is derived from the result of Ref. [20] which treats the discrete levels and the continuum states on the basis of an ion-sphere model.

According to Eq. (3), an excited-level population in QSS consists of two components: the second term is called the ionizing plasma component and the first the recombining plasma component [4]. It turned out useful to treat these two components separately and to examine the population kinetics for each of these two components [5–7]. Following this spirit we solve the set of the rate equations under the conditions corresponding to these cases; under the ionizing plasma condition $n(1)$ is kept constant and n_z is set equal to zero, and vice versa under the recombining plasma condition.

A. Ionizing plasma

The condition for calculation is that for $t<0$, populations of excited levels are zero, which may correspond to $n(1)=0$ or $n_e=0$ or $T_e=0$, and at $t=0$ an abrupt change takes place to constant values of $n(1)=1$ cm^{-3}, $n_e=10^{12}$ cm^{-3}, and $T_e=10$ eV. This latter condition corresponds to a high temperature case of ionizing plasma [5]. In the calculation, we assume that the population density divided by the statistical weight for higher-lying levels with $p \ge 36$ is proportional to p^{-6} starting from $p=35$ [5,21]. The validity of this approximation will be discussed later.

Figure 1(a) shows the transient populations, where population of excited levels has been divided by its statistical weight $g(p)$. The thin dashed lines show the result of the QSS, which is the final value of the transient populations. Figure 1(b) is another plot of Fig. 1(a). The QSS values are shown with the closed circles. It can be seen that for $t < 1\times10^{-9}$ sec all $n(p)$ in Fig. 1(a) are proportional to t, and $n(p)/g(p)$ is approximately proportional to p^{-5} [Fig. 1(b)]. For $t > 1\times10^{-9}$ sec, with the course of time, level 2 reaches its final value first, level 3 second, and then level 4. At $t \simeq 1\times10^{-7}$ sec, all the higher-lying levels $p \ge 5$ reach the final values at the same time. We define the *transient time* $\tau_{tr}(p)$ at which, in Fig. 1(a), the transient population reaches 63% of its final steady-state value. In Fig. 2, $\tau_{tr}(p)$ for each level is shown with the crosses. We define the response time τ_{res}, which is the largest among $\tau_{tr}(p)$'s.

Figure 3(a) shows the dominant flows of electrons in the simplified energy level diagram at $t=1\times10^{-9}$ sec. From $t=0$ to 1×10^{-9} sec, the dominant populating process of all the levels is the direct excitation from the ground state and depopulation is insignificant (compare the corresponding flows). This means that, in this period, the population is simply accumulating without depopulation. Therefore the populations of the excited levels are approximated by

$$n(p) = C(1,p) n_e t . \tag{6}$$

As we have seen, $n(p)/g(p)$ is approximately proportional to p^{-5}. This is in accordance with the above populating mechanism; i.e., $C(1,p) \propto p^{-3}$ for large p. This last

relation stems from the p dependence of the absorption oscillator strengths.

Figure 2 shows the depopulating rate by electron collisions and that by radiative transitions. Levels $p=4$ or 5 establish the boundary between the higher-lying levels, for which the electron collisional depopulation is dominant, and the lower-lying levels, for which the radiative decay is dominant. The level is called Griem's boundary, p_G [5,6,22]. In the present case $p_G \simeq 4.5$.

For a lower level than p_G, Eq. (1) can be approximated by

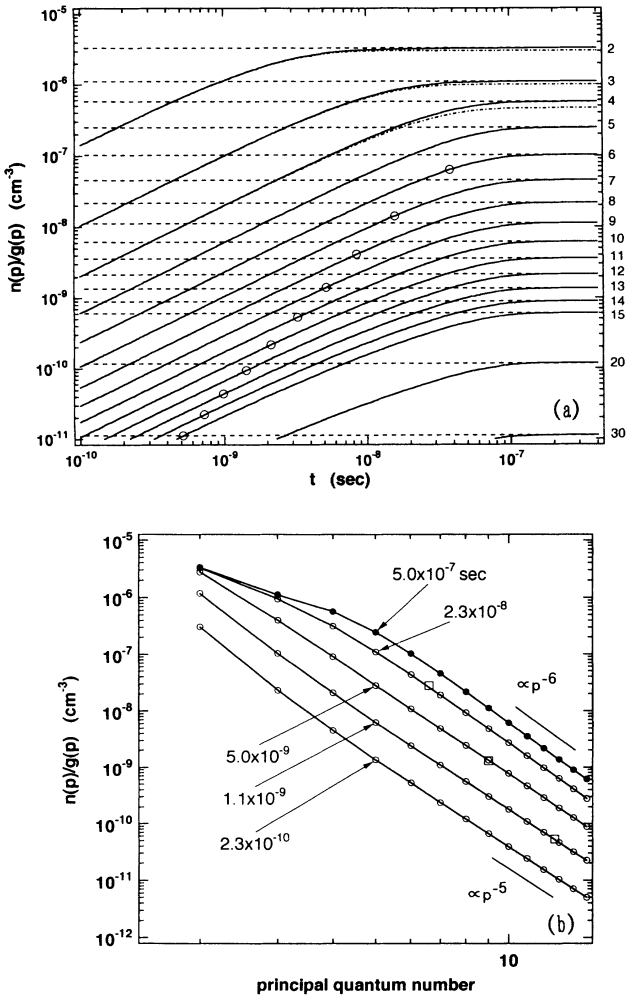

FIG. 1. (a) Transient populations of excited hydrogen atoms under the ionizing plasma condition for $T_e=10$ eV, $n_e=10^{12}$ cm^{-3}, and $n(1)=1$ cm^{-3}. Population density has been divided by the statistical weight. The numbers at right denote p. Dashed line: the QSS values. Dash-and-dotted line: Eq. (8). Open circle: the time at which the populating mechanism of the level changes from the direct excitation to the excitation from the adjacent lower-lying level, or the ladderlike excitation. (b) Temporal development of the population density distribution. Closed circle: QSS values. Square: the levels undergoing the transition in populating process. Levels lying lower than this have $n(p)/g(p) \propto p^{-5}$ and those higher than this have $n(p)/g(p) \propto p^{-6}$. Time t (sec) is indicated in the figure.

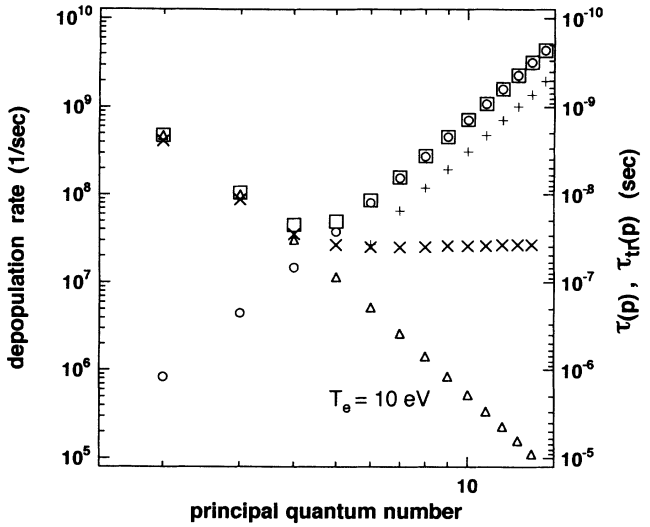

FIG. 2. Depopulating rates for $T_e=10$ eV and $n_e=10^{12}$ cm^{-3}. Triangle: radiative decay rate; circle: total collisional depopulation rate. Among the collisional rates the dominant one is the excitation to the adjacent higher-lying level. Square: sum of these rates which is the inverse relaxation time $\tau(p)^{-1}$. Cross: transient time $\tau_{tr}(p)$ determined from Fig. 1(a). Plus: the time when the transition, Eq. (9), takes place. These times refer to the right-hand side ordinate.

$$dn(p)/dt = C(1,p)n_e n(1) - \sum_{q<p} A(p,q)n(p) \ . \tag{7}$$

This is readily solved as

$$n(p) = \left[C(1,p)n_e n(1) \Big/ \sum_{q<p} A(p,q) \right] \times \left[1 - \exp\left[- \sum_{q<p} A(p,q)t \right] \right] \ . \tag{8}$$

The dash-and-dotted curves in Fig. 1(a) indicate Eq. (8). Slight differences at the final steady state come from the neglect of the cascading effect in Eq. (7). For these levels, $\tau_{tr}(p)$ is given by $[\sum_{q<p} A(p,q)]^{-1}$.

Figures 1 and 2 show that levels higher than p_G have a common $\tau_{tr}(p)$. For $t > 1\times10^{-9}$ sec, populations of excited levels become higher, and the populating process of levels higher lying than p_G changes from direct excitation [Fig. 3(a)] to the excitation from the adjacent lower-lying level as seen in Fig. 3(b), which shows dominant flows of electrons at the final steady state. With an increase in t this change takes place from higher-lying levels. In Figs. 1(a) and 2 the time of this transition or the level which is undergoing this transition is plotted. At the time of the transition of level p,

$$n(p-1)C(p-1,p)n_e = n(1)C(1,p)n_e \tag{9}$$

holds. At this time, level $(p-1)$ is still in the initial phase, Eq. (6),

$$C(1,p-1)n(1)n_e tC(p-1,p)n_e = n(1)C(1,p)n_e \ . \tag{10}$$

This is readily solved for t,

$$t = C(1,p)/[C(1,p-1)C(p-1,p)n_e] \sim [p/(p-1)]^{-3}/[C(p-1,p)n_e] , \quad (11)$$

where use has been made of the relation $C(1,p) \propto p^{-3}$ for large p. With the aid of the relation $C(p,p+1) \propto p^4$ [5], Eq. (11) is approximated to

$$t \approx 1/[C(p,p+1)n_e] . \quad (12)$$

Remembering the fact that the dominant depopulating process of these levels is the excitation to the adjacent higher-lying level, we obtain $t \approx \tau(p)$. Figure 2 shows this approximate relationship to be valid within a factor of 2. At a given time, the ladderlike excitation mechanism is established among all the levels lying higher than the level which is undergoing this transition, and their populations are determined by the population of this lower end of the excitation ladder. This is because the relaxation time for $p \geq p_G$ is shorter for larger principal quantum numbers as shown in Fig. 2. Therefore these populations appear in Fig. 1(a) as strictly parallel and in Fig. 1(b) proportional to p^{-6}. It is concluded from the reasoning in [5] that the lowest level that undergoes this transition is approximately equal to Griem's boundary level, p_G. This is the reason why levels $p \geq p_G$ have the common $\tau_{tr}(p)$ and why this is given by $\tau_{tr}(p_G)$, or the maximum of $\tau(p)$'s (see Fig. 2).

The approximation of $n(p)/g(p)$ for $p \geq 36$ adopted in our calculation is thus exact for $t \geq 10^{-11}$ sec and is reasonably good at earlier times because, under the ionizing plasma condition, the cascading effect is insignificant and a small error in $n(p)$ ($\propto p^{-5}$ or p^{-6}) for $p \geq 36$ would result in no serious error in $n(p)$ of our interest.

Figure 4 shows the effective depletion rate coefficient of $n(1)$ and the production rate coefficient of n_z. The difference between these rate coefficients is the production rate coefficient of total populations of excited levels. The depletion rate coefficient at $t=0$ is equal to the sum of the excitation and ionization rate coefficients. With an increase in t, populations of the excited levels increase (Fig. 1) and thus the returning electron flows into the ground state increase [Fig. 3(b)]. Accordingly, the effective depletion rate coefficient decreases. The amount of this decrease ($\simeq 1.3\times10^{-8}$ cm^3 sec^{-1}) is approximately equal to $\sum_{p<p_G} C(1,p)$ ($\simeq 1.4\times10^{-8}$ cm^3 sec^{-1} with $p_G \simeq 4.5$). The production rate coefficient of n_z at $t=0$ is nothing but the direct ionization rate coefficient. The increase in the populations of excited levels with t (Fig. 1) results in the slight increase in the rate coefficient. The magnitude of this increase ($\simeq 0.9\times10^{-9}$ cm^3 sec^{-1}) is given by the ladderlike excitation ionization and is ap-

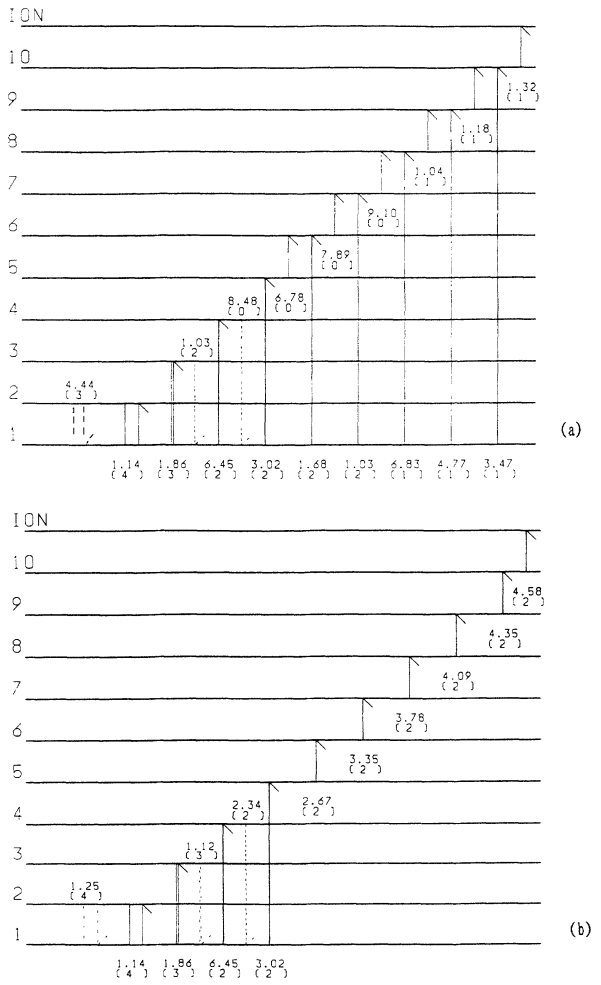

FIG. 3. For each level the largest populating flow to this level and the largest depopulating flow from this level are given. The solid arrow is for the collisional transition, and the dashed one the radiative transition. The number attached to the arrow indicates the magnitude of the flow, where 4.44 (3) should read 4.44×10^3 cm^{-3} sec^{-1}. Level "ION" denotes free electron level and $11 \leq p \leq 35$. (a) At 1×10^{-9} sec. (b) At 5×10^{-7} sec.

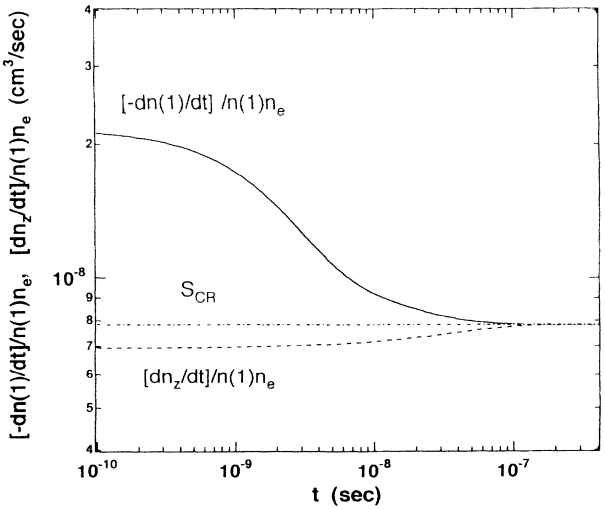

FIG. 4. Effective depletion rate coefficient of $n(1)$ $[-dn(1)/dt]/n(1)n_e$ and production rate coefficient of n_z $[dn_z/dt]/n(1)n_e$. S_{CR} is also shown. In our calculation, $n(1)$ and n_z are assumed constant. This is equivalent to assuming that the lost $n(1)$ is supplied and the produced n_z is removed.

proximately equal to $\sum_{p>p_G} C(1,p)$ ($\simeq 0.9\times10^{-9}$ $cm^3\,sec^{-1}$). Finally, at $t\approx\tau_{res}$ these two rate coefficients agree with S_{CR}. The values of the depletion and production rate coefficients at $t=0$ are independent of n_e. S_{CR} takes a value between these coefficients and its dependence on n_e is through the n_e dependence of p_G. For the low density limit, for example, S_{CR} is given by the direct ionization rate coefficient. For high density limit, S_{CR} is approximated to $[\sum_{p\geq 2} C(1,p)+S(1)]\approx C(1,2)$ [8].

B. Recombining plasma

The condition for calculation is that before $t=0$, populations of excited levels are zero, which means $n_z=0$ or $n_e=0$ or $T_e=\infty$, and at $t=0$, an abrupt change takes place to constant values of $n_z=1$ cm^{-3}, $n_e=10^{12}$ cm^{-3}, and $T_e=0.1$ eV. This condition corresponds to a low temperature case of a recombining plasma [7]. Results for a high temperature case will be shown in Appendix A. We approximate the population density of higher levels with $36\leq p\leq 76$ by

$$n(p)=\alpha(p)n_e^2 n_z t\ , \tag{13}$$

until it reaches the final steady-state value Figures 5(a) and 5(b) show transient characteristics of the population densities. Dashed lines in Fig. 5(a) and the closed circles in Fig. 5(b) show the QSS values. In Fig. 5(b) the Saha-Boltzmann local thermodynamic equilibrium (LTE) populations are given with the squares. Figure 6 shows $\tau_{tr}(p)$ determined from Fig. 5(a) together with the collisional and radiative depopulation rates and $\tau(p)$.

We now examine the transient population. Figure 7 shows the rate coefficients for radiative recombination and three-body recombination. For levels $p>4$ the three-body recombination dominates over the radiative recombination, which in turn is dominant for $p<4$. In the early times of $t\leq 10^{-10}$ sec the population density distribution in Fig. 5(b) directly reflects Fig. 7, suggesting that the dominant populating process is the direct recombination. Remember that in Fig. 5(b) the population has been divided by the statistical weight. This is actually seen in the dominant flow diagram of electrons in Fig. 8(a) and is consistent with $n(p)\propto t$ in Fig. 5(a). In this figure the dash-dotted lines show Eq. (13). It may be interesting to note that population inversion is established for $p>4$ because of the p dependence of $\alpha(p)\propto p^6$.

With an increase in t the populations of levels $p>4$ deviate upward from Eq. (13), and they reach the final QSS values starting from the higher-lying levels However, $\tau_{tr}(p)$ is appreciably longer than $\tau(p)$ as seen in Fig. 6. These two observations are explained from the fact that these high-lying levels, when their populations are close

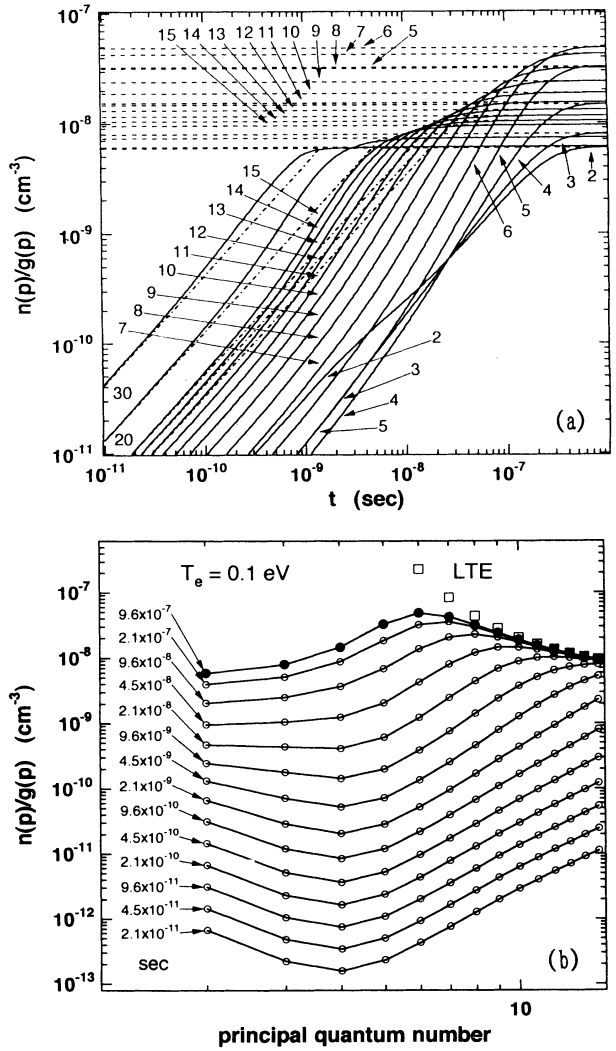

FIG. 5. (a) Transient populations of excited hydrogen atoms under the recombining plasma condition of $T_e=0.1$ eV, $n_e=10^{12}$ cm^{-3}, and $n_z=1$ cm^{-3}. Dashed line: QSS population. Dash-and-dotted line: Eq. (13). (b) Temporal development of the population density distribution. Closed circles indicate the QSS values. Square: LTE population.

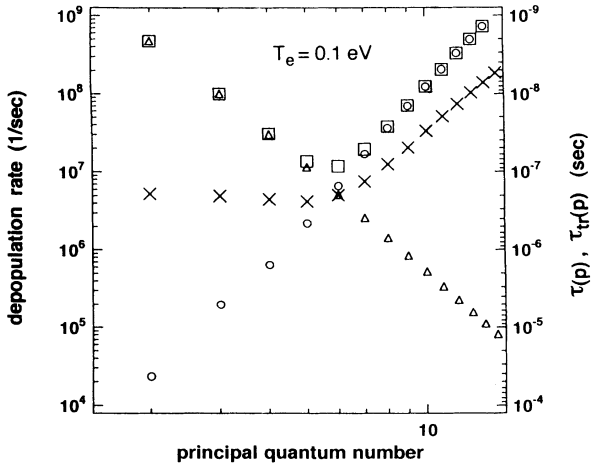

FIG. 6. Depopulating rates $\tau(p)$ and $\tau_{tr}(p)$ for the recombining plasma. See Fig. 2 for notations. Griem's boundary is level 6. Byron's boundary lies between levels 6 and 7; the dominant depopulating collisional transition for higher-lying levels is the excitation to the adjacent higher-lying level, and for the lower-lying level is the deexcitation to the adjacent lower-lying level.

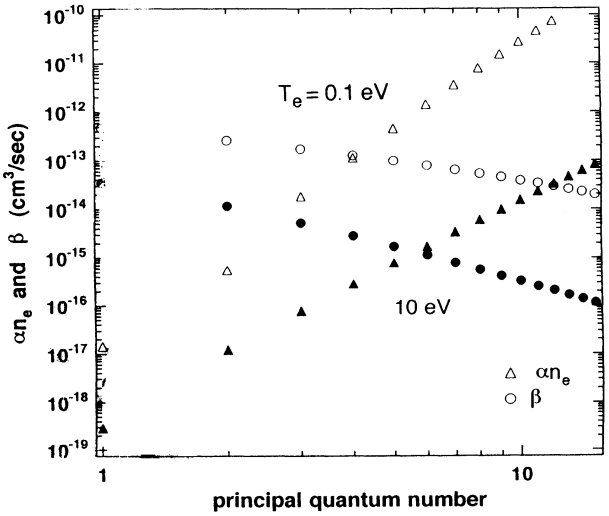

FIG. 7. Rate coefficient for three-body recombination multiplied by $n_e = 10^{12}$ cm^{-3} and that for radiative recombination. For $T_e = 10$ eV approximate relations $\alpha(p) \propto p^4$ and $\beta(p) \propto \ln p / p^3 \approx$ hold. For $T_e = 0.1$ eV, $\alpha(p) \propto p^6$ and $\beta(p) \propto p$.

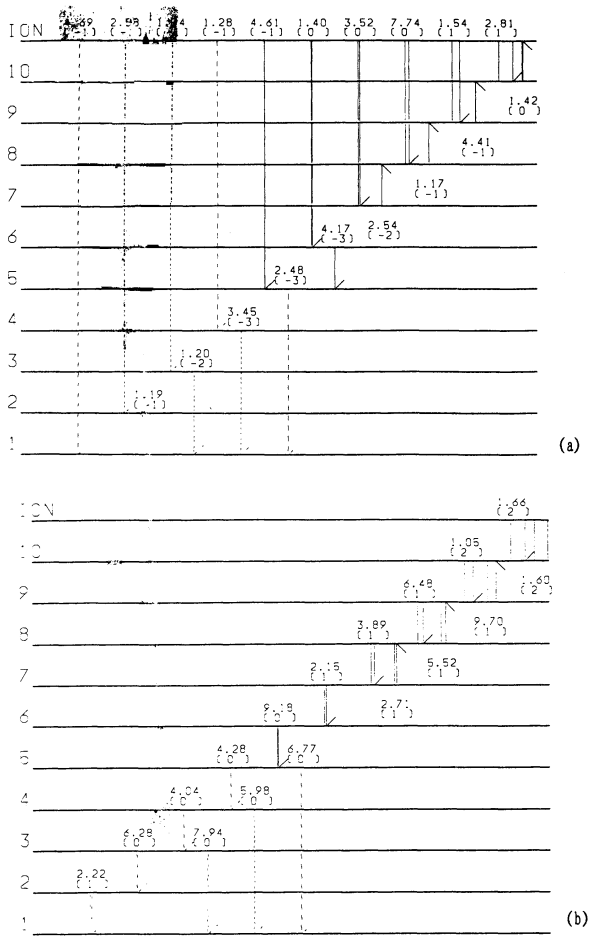

FIG. 8. Flow diagram similar to Fig. 3 for the recombining plasma. See Fig. 3 for notations. (a) At $t = 1 \times 10^{-9}$ sec. (b) At $t = 1 \times 10^{-6}$ sec.

to the QSS or LTE values, are strongly coupled to each other by collisional transitions. This is seen in Fig. 8(b). As a result, a level, when its population is lower than the LTE values, receives additional populating flow from the neighboring higher-lying levels, or it is "pulled" upward toward its LTE value. Level p reaches its final value only when deexcitation flow from this level to the adjacent lower-lying level $(p-1)$ is balanced by the excitation flow from $(p-1)$ to p. In other words, when the population of a level is close to the LTE value, it is "pulled" downward by the lower-lying levels which are still far from LTE.

Among lower-lying levels, but still higher than p_G, there is a boundary level, Byron's boundary [7] p_B; for levels lying higher than this the excitation rate from this level is larger than the deexcitation rate and for levels lying lower than this the situation is reversed. In the present example this level, which is approximately given by $(13.6/3kT_e)^{1/2}$ [7], is between $p = 6$ and 7 (see Fig. 8). For levels lower than p_B (and still higher than p_G), the collisional coupling becomes only downward and the population of a level is controlled by that of the adjacent higher-lying level. It might thus be assumed that $\tau_{tr}(p)$ for these levels, as in the ionizing plasma case, is given by $\tau_{tr}(p_B)$. It turns out not to be the case. This is because lower levels have longer $\tau(p)$'s and lag behind p_B.

In Fig. 5(a) the slope of the population of level 2 deviates downward from the linear relationship, Eq. (13) with the $\alpha(p)n_e$ replaced by $\beta(p)$, at $t \simeq 2 \times 10^{-9}$ sec, which corresponds to $\tau(2)$. If the cascading contributions from levels $p > 2$ were absent, the population would have reached a final value at this time. In fact, the cascading contributions are substantial and even dominant at later times. Depending on the time dependence of populations of the levels that contribute to the cascading population of level 2, its population increases with time. A similar, but less prominent, feature is seen with level 3. This is the reason these lower-lying levels cannot reach their

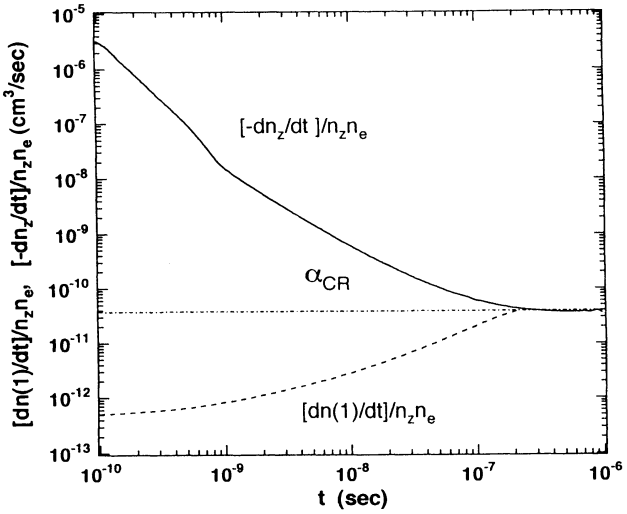

FIG. 9. Effective depletion rate coefficient of n_z $[-dn_z/dt]/n_z n_e$ and production rate coefficient of $n(1)$ $[dn(1)/dt]/n_z n_e$. α_{CR} is also shown.

QSS values until Griem's boundary level $p_G=6$, which has the largest $\tau(p)$, reaches its QSS value (see Fig. 6).

Figure 9 shows effective depletion rate coefficient of n_z and production rate coefficient of $n(1)$. The difference between these rate coefficients is the production rate coefficient of total populations of excited levels. At $t=0$, the depletion rate coefficient diverges because of the p^6 dependence of $\alpha(p)$, but the production rate coefficient is equal to $\alpha(1)n_e+\beta(1)$. With an increase in t, populations of the excited levels enter into Saha-Boltzmann equilibrium starting from higher-lying levels (Fig. 5), and the returning ionization flows balance with the recombination flows [Fig. 8(b)], making the effective depletion rate coefficient decrease. The increase in the populations of excited levels with t results in the increase in the production rate coefficient. The magnitude of this increase ($\simeq 4\times 10^{-11}$ cm^3 sec^{-1}) is given approximately by $\sum_{p<p_G} A(p,1)n(p)/n_z n_e$ with $p_G\simeq 6$, or by $n(p_B)F(p_B,p_B-1)/n_z$ with $p_B\simeq 7$. The latter quantity is 2×10^{-11} cm^3 sec^{-1} [see Fig. 8(b)]. Finally, for $t\geq\tau_{\rm res}\simeq 3\times 10^{-7}$ sec, the effective depletion rate coefficient and the effective production rate coefficient agree with $\alpha_{\rm CR}$.

III. CONCLUSION AND DISCUSSION

We have shown that, for both the ionizing plasma condition and the recombining plasma condition, the overall response time of the system of excited levels is given by the transient time of Griem's boundary level $\tau_{\rm tr}(p_G)$, which is equal to the longest relaxation time among $\tau(p)$.

In our calculation we took as an example $T_e=10$ eV and $n_e=10^{12}$ cm^{-3} for the ionizing plasma condition and $T_e=0.1$ eV and $n_e=10^{12}$ cm^{-3} for the recombining plasma condition. Griem's boundary p_G depends on n_e and, to a lesser extent, on T_e. Figure 10(a) shows the boundary for a broad range of plasma parameter. Figure 10(b) shows the relaxation time of the boundary together with the response time as determined from Fig. 2 or 6 and similarly for other conditions.

We consider the validity of the QSS. First we assume n_e and T_e are fixed, so that $\tau_{\rm res}$ is constant. We have shown that if the transient population of level p_G, which determines $\tau_{\rm res}$, reaches its QSS values, QSS is valid for all the excited levels. We examine a temporal change in $n(1)$ for ionizing plasma. The temporal development of the population of level p_G is approximately expressed by [see Fig. 1(a)]

$$dn(t)/dt=C(1,p_G)n_e N(t)-\tau_{\rm res}^{-1}n(t)\ , \tag{14}$$

where $n(t)$ and $N(t)$ stand for $n(p_G)$ and $n(1)$, respectively, at t. In the QSS approximation, the time derivative is set equal to zero and the population is given as

$$n(t)_{\rm CR}=\tau_{\rm res}C(1,p_G)n_e N(t)\ . \tag{15}$$

We assume that the temporal change of $N(t)$ is expressed in terms of a time constant T as

$$N(t)=N_0\exp(-t/T)\ , \tag{16}$$

where N_0 is the initial value and T is positive for decreasing $N(t)$ and negative for increasing $N(t)$. For t and $|T|\gg\tau_{\rm res}$, Eqs. (14)–(16) lead to

$$n(t)_{\rm CR}/n(t)=[T-\tau_{\rm res}]/T\ . \tag{17}$$

This relation indicates that the parameter $(\tau_{\rm res}/T)$ gives a measure of deviation of the CR population from its actual value. Thus the validity condition of QSS is that

$$|\tau_{\rm res}/T|\ll 1\ . \tag{18}$$

Next we examine a temporal change in n_z for recombining plasma. The dominant populating flow of level p_G is deexcitation from the adjacent higher-lying level. We now take into account "the time lag" of this population. Then the population of p_G is approximately given as

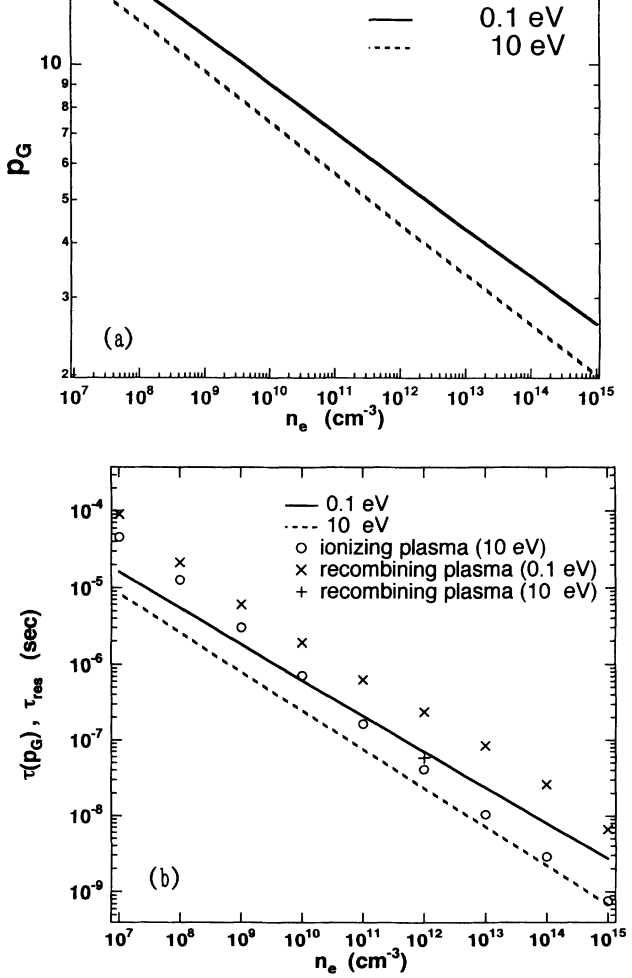

FIG. 10. (a) Griem's boundary p_G for $T_e=0.1$ and 10 eV. (b) The relaxation time of Griem's boundary; this corresponds to the overall response time of the system of the excited levels. Open circle: $\tau_{\rm res}$ for the ionizing plasma with $T_e=10$ eV determined from calculation similar to Fig. 1. Cross: corresponding result for the recombining plasma with $T_e=0.1$ eV. Plus: similar result for $T_e=10$ eV.

$$dn(t)/dt = F(p_G+1,p_G)n_e R_0(p_G+1)N(t-\tau_{\rm res})n_e - \tau_{\rm res}^{-1}n(t) , \quad (19)$$

where $N(t)$ is the ion density in this case at t. In the QSS approximation, the population of p_G is expressed as

$$n(t)_{\rm CR} = \tau_{\rm res}F(p_G+1,p_G)n_e R_0(p_G+1)N(t)n_e . \quad (20)$$

If $N(t)$ is again expressed by Eq. (16), then Eqs. (18)–(20) lead to

$$n(t)_{\rm CR}/n(t) = \exp(-\tau_{\rm res}/T)[T-\tau_{\rm res}]/T \quad (21)$$

for t and $|T| \gg \tau_{\rm res}$. The validity condition of QSS is again given by Eq. (18).

When n_e changes with time, we may start with Eq. (14) or Eq. (19). Instead of $N(t)$ or $N(t-\tau_{\rm res})$, the factor n_e changes now. We may proceed with our discussion in a similar way to the above cases. We then reach the same conclusion as for the previous cases. The change in p_G or $\tau_{\rm res}$ with the change in n_e, which we have neglected so far, affects little in the above reasoning. This is because $n(p_G)$ is almost linearly dependent on n_e.

The case of a temporal change in T_e is not straightforward because the collision rates have nonlinear dependence on T_e. First we examine ionizing plasma and start with Eq. (14). Instead of the change in $N(t)$, $C(1,p_G)$ changes this time. When we note that $\tau_{\rm res}$ is very weakly dependent on T_e, we can proceed with our discussion in much the same way as for the previous cases. Validity of the QSS would then be $|\tau_{\rm res}dC(1,p_G)/dt/C(1,p_G)| \ll 1$. The excitation rate coefficient $C(1,p_G)$ may be approximated as

$$C(1,p_G) = \text{const} \times T_e^{-0.5}\exp[-E(1,p_G)/kT_e] , \quad (22)$$

where $E(1,p_G)$ is the excitation energy of p_G from the ground state. Except for very high temperature, the temperature dependence of Eq. (22) is mainly determined by the exponential factor and the $T_e^{-0.5}$ factor may be neglected. Then the validity condition is written as

$$|(\tau_{\rm res}/T)E(1,p_G)/kT_e| \ll 1 , \quad (23)$$

where T is the time constant of the change in T_e. For recombining plasma, except for the case of $p_G < p_B$, i.e., low temperature and high density, the QSS value of $n(p_G)$ is approximately given by its LTE value,

$$n(t)_{\rm CR} \simeq Z(p_G)n_z n_e . \quad (24)$$

Here the Saha-Boltzmann coefficient is

$$Z(p_G) = g(p_G)/2[h^2/(2\pi mkT_e)]^{3/2}\exp[\chi(p_G)/kT_e] , \quad (25)$$

where $g(p_G)$ and $\chi(p_G)$ are, respectively, the statistical weight and the ionization potential of level p_G, and the other symbols have the usual meanings. Equation (24) suggests that the validity condition for QSS would be given by

$$|\tau_{\rm res}dZ(p_G)/dt/Z(p_G)| \ll 1 . \quad (26)$$

If the above conditions are satisfied, the validity condition Eq. (5), which was proposed by Bates *et al.*, may not be necessary. In fact, the ionizing plasma and the recombining plasma violate this condition but we cannot find any reason that QSS cannot be applied to these plasmas. Their third statement, in particular, is concerned with the existence of the level itself [20], not with the QSS approximation.

For other hydrogenic ions, the foregoing results can be applied on the basis of the scaling summarized in Appendix B.

ACKNOWLEDGMENTS

This work is part of a joint research program on the WT-3 tokamak, Department of Physics, Kyoto University. This work is partly supported by the Japan Society for the Promotion of Science.

APPENDIX A: HIGH TEMPERATURE CASE FOR RECOMBINING PLASMA

For a high temperature recombining plasma, which may be important for very high z ions [3,8,18], the magnitude and the p dependence of the recombination rate coefficients are different from those for the low temperature case as seen in Fig. 7. Figure 11 shows the transient population distribution for $T_e = 10$ eV. The initial distributions are appreciably different from those in Fig. 5(b) because of the different p dependences of $\beta(p)$ and $\alpha(p)$. It is also noted that the population inversion among the levels $p < p_G$ has disappeared. This is also explained by the p dependence of $\beta(p)$.

APPENDIX B: SCALING LAW FOR HYDROGENLIKE IONS

Atomic parameters for hydrogenlike ions follow scaling laws depending on the nuclear charge z.

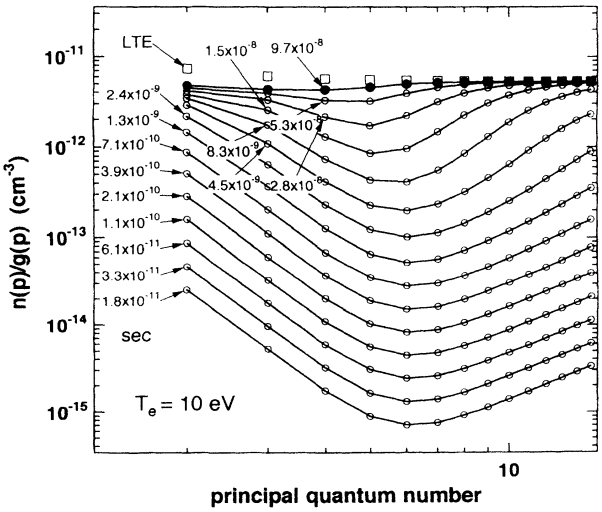

FIG. 11. Temporal development of the population density distribution similar to Fig. 5(b), but $T_e = 10$ eV, the high temperature case.

$$A(p,q)=z^4 A(p,q)^{\mathrm{H}} , \tag{B1}$$

where the superscript H indicates the quantity for neutral hydrogen. If we scale T_e according to

$$T_e=z^2 T_e^{\mathrm{H}} , \tag{B2}$$

collision rate coefficients approximately scale as

$$C(q,p)=z^{-3}C(q,p)^{\mathrm{H}} , \tag{B3}$$

$$F(p,q)=z^{-3}F(p,q)^{\mathrm{H}} , \tag{B4}$$

$$S(p)=z^{-3}S(p)^{\mathrm{H}} , \tag{B5}$$

$$\alpha(p)=z^{-6}\alpha(p)^{\mathrm{H}} , \tag{B6}$$

$$\beta(p)=z\beta(p)^{\mathrm{H}} . \tag{B7}$$

The z scaling of the right-hand side of Eq. (1) can be simplified if we adopt

$$n_e=z^7 n_e^{\mathrm{H}} , \tag{B8}$$

$$n_z=z^{-4}n_z^{\mathrm{H}} . \tag{B9}$$

The above scaling laws, as applied to the right-hand side of Eq. (1), result in z^4 scaling. This results in the scaling for t,

$$t=z^{-4}t^{\mathrm{H}} . \tag{B10}$$

In our preceding results parameters should be understood to have the superscript H; for example, t in Fig. 1 is t^{H}. If we intend to apply our present result to, for example, $z=10$ hydrogenlike neon, the following procedure should be applied: $T_e=10^2\times 10$ eV, $n_e=10^7\times 10^{12}$ cm^{-3}, $t=10^{-4}\,t^{\mathrm{H}}$ sec.

For recombining plasma, instead of the scaling (B9) and (B10), we may adopt another scaling;

$$n_z=n_z^{\mathrm{H}} \text{ and } t=z^{-8}t^{\mathrm{H}} . \tag{B11}$$

Finally, we give a few examples of the actual scaling in our figures for the case of $z=10$; in Fig. 1(a) $t=10^{-10}$ sec should read 10^{-14} sec. In Fig. 2 rate 10^5 sec^{-1} should read 10^9 sec^{-1}. In Fig. 4 rate coefficient 10^{-8} (cm^3/sec) should read 10^{-11} (cm^3/sec). In Fig. 7 rate coefficient 10^{-19} (cm^3/sec) should read 10^{-18} (cm^3/sec). In Fig. 9 rate coefficient 10^{-13} (cm^3/sec) should read 10^{-12} (cm^3/sec), where we use Eq. (B9).

[1] D. R. Bates, A. E. Kingston, and R. W. P. McWhirter, Proc. R. Soc. London **267**, 297 (1962).
[2] D. R. Bates and A. E. Kingston, Planet. Space Sci. **11**, 1 (1963).
[3] R. W. P. McWhirter and A. G. Hearn, Proc. Phys. Soc. London **82**, 641 (1963).
[4] T. Fujimoto, J. Phys. Soc. Jpn. **47**, 265 (1979).
[5] T. Fujimoto, J. Phys. Soc. Jpn. **47**, 273 (1979).
[6] T. Fujimoto, J. Phys. Soc. Jpn. **49**, 1561 (1980).
[7] T. Fujimoto, J. Phys. Soc. Jpn. **49**, 1569 (1980).
[8] T. Fujimoto, J. Phys. Soc. Jpn. **54**, 2905 (1985).
[9] C. C. Limbaugh and A. A. Mason, Phys. Rev. A **4**, 2368 (1971).
[10] J. Peyraud and N. Peyraud, J. Appl. Phys. **43**, 2993 (1972).
[11] J. M. Green and W. T. Silfvast, Appl. Phys. Lett. **28**, 253 (1976).
[12] W. W. Jones and A. W. Ali, Appl. Phys. Lett. **26**, 450 (1975).
[13] G. J. Pert, J. Phys. B **9**, 3301 (1976).
[14] G. J. Tallents, J. Phys. B **10**, 1769 (1977).
[15] S. Suckewer and H. Fishman, J. Appl. Phys. **51**, 1922 (1980).
[16] N. H. Burnett and G. D. Enright, IEEE J. Quantum Electron. **26**, 1798 (1990).
[17] L. I. Gudzenko, L. A. Shelepin, and S. I. Yakovlenko, Usp. Fiz. Nauk **114**, 457 (1974) [Sov. Phys. Usp. **17**, 848 (1975)].
[18] T. Fujimoto and R. W. P. McWhirter, Phys. Rev. A **42**, 6588 (1990).
[19] K. Sawada, K. Eriguchi, and T. Fujimoto, J. Appl. Phys. **73**, 8122 (1993).
[20] I. Shimamura and T. Fujimoto, Phys. Rev. A **42**, 2346 (1990).
[21] D. A. Benoy, J. A. M. van der Mullen, B. van der Sijde, and D. C. Schram, J. Quant. Spectrosc. Radiat. Transfer **46**, 195 (1991).
[22] H. R. Griem, *Plasma Spectroscopy* (McGraw-Hill, New York, 1964).